

Supporting Information

Supramolecular Copolymerization as a Strategy to Control the Stability of Self-Assembled Nanofibers

Bala N. S. Thota, Xianwen Lou, Davide Bochicchio, Tim F. E. Paffen, René P. M. Lafleur, Joost L. J. van Dongen, Svenja Ehrmann, Rainer Haag, Giovanni M. Pavan, Anja R. A. Palmans, and E. W. Meijer**

anie_201802238_sm_miscellaneous_information.pdf

Content:

1. Materials and methods	S2
2. Synthetic procedures	S4
3. Supplementary Figures, Schemes and Tables	S13
4. Preparation procedure for aqueous BTA samples	S24
5. HDX measurements	S24
6. Fit Procedures	S25
7. Matlab script for tri-exponential curve fitting of HDX decay data	S25
8. Molecular Dynamics Simulations	S29
9. References	S30

1. Materials and methods:

Unless stated otherwise, all reagents and chemicals were obtained from commercial sources at the highest purity available and used without further purification. All solvents were of AR quality and purchased from Biosolve. Water was purified on an EMD Milipore Mili-Q Integral Water Purification System. Reactions were followed by thin-layer chromatography (precoated 0.25 mm, 60-F254 silica gel plates from Merck), and flash chromatography was run with silica gel (40–63 μm , 60 Å from Screening Devices b.v.). Dry solvents were obtained with an MBRAUN Solvent Purification System (MB-SPS). Automated column chromatography was conducted on a Grace Reveleris X2 Flash Chromatography System using Reveleris Silica Flash Cartridges. 1-Phenyl-2,5,8,11,14-pentaoxahexacosan-26-amine¹ and compounds **7**,² **8**² and **nBTA**¹ were synthesized according to literature procedures.

NMR spectra were recorded on Bruker 400 MHz Ultrashield spectrometers (400 MHz for ¹H NMR). Deuterated solvents used are indicated in each case. Chemical shifts (δ) are expressed in ppm and are referred to the residual peak of the solvent. Peak multiplicity is abbreviated as s: singlet; d: doublet; t: triplet; dt: doublet of triplets; ddt: doublet of doublets of triplets; td: triplet of doublets; tt: triplet of triplets; q: quartet; qd: quartet of doublets; m: multiplet.

Matrix assisted laser absorption/ionization-time of flight (MALDI-TOF) mass spectra were obtained on a PerSeptive Biosystems Voyager DE-PRO spectrometer using α -cyano-4-hydroxycinnamic acid (CHCA) or *trans*-2-[3-(4-*tert*-butylphenyl)-2-methyl-2-propenylidene]-malononitrile (DCTB) as matrix.

Infrared spectroscopy measurements were performed on a Perkin Elmer FT-IR Spectrum Two apparatus. Solution FT-IR measurements were performed using a CaF₂ Liquid Cell with 0.05 mm path length purchased from New Era Enterprises.

Ultraviolet-visible (UV-vis) absorbance spectra were recorded on and a Jasco V-650 UV-vis spectrometer with a Jasco ETCT-762 temperature controller.

Transmission electron microscopy was performed using a Tecnai Sphera microscope equipped with a LaB6 filament operating at 200 kV and a bottom mounted 1024x1024 Gatan charge-couple device (CCD) camera. TEM samples were prepared by drop casting 10 μL of the sample solution (0.2 mM) on a TEM grid, which was surface plasma treated just prior to use (Cressington 208 carbon coater operating at 5 mA for 40 s). Excess sample was removed by blotting using a filter paper. The grids were dried at room temperature for 4-5 h, followed by drying in a vacuum desiccator overnight. The BTA concentration in the samples was 200 μM .

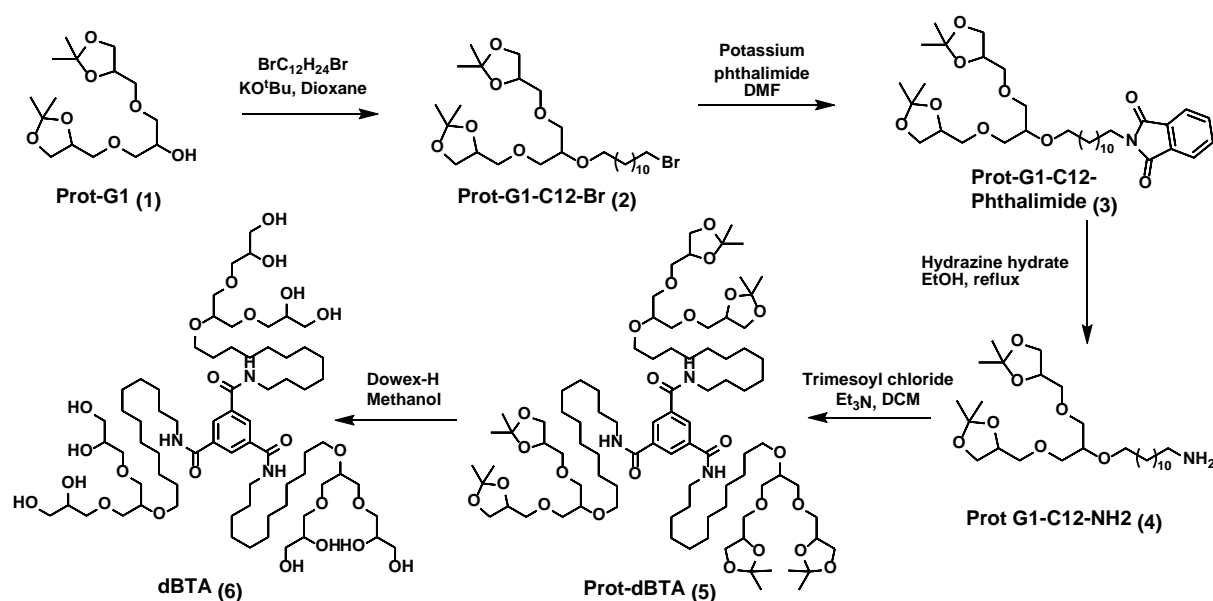
Cryogenic transmission electron microscopy was performed on samples with a concentration of 586 μM for **nBTA** and 1 mM for **dBTA** and **nBTA/dBTA** mixtures. Vitrified films were prepared

in a 'Vitrobot' instrument (PC controlled vitrification robot, patent applied, Frederik et al 2002, patent licensed to FEI) at 22°C and a humidity of 100%. In the preparation chamber of the 'Vitrobot' a 3 μ L sample was applied on a Quantifoil grid (R 2/2, Quantifoil Micro Tools GmbH), which was surface plasma treated just prior to use (Cressington 208 carbon coater operating at 5 mA for 40 s). Excess sample was removed by blotting using two filter papers for 3 s at –3 mm, and the thin film thus formed was shot (acceleration about 3 g) into liquid ethane just above its freezing point. The vitrified film was transferred to a cryoholder (Gatan 626) and observed at –170 °C in a Tecnai Sphera microscope operating at 200 kV. Microscopy images were taken at low dose conditions and at a defocus of 10 μ m (magnification: 25000). The BTA concentration in the samples was 586 μ M for nBTA and 1 mM for dBTA and nBTA/dBTA mixtures.

Dynamic light scattering measurements were recorded on an ALV/CGS-3 MD-4 compact goniometer system equipped with a multiple tau digital real time correlator (ALV-7004) and a solid state laser ($\lambda = 532$ nm; 40 mW).

HDX-MS measurements were carried out using a Xevo™ G2 QTof mass spectrometer (Waters) with a capillary voltage of 2.7 kV and a cone voltage of 20 V. The source temperature was set at 100°C, the desolvation temperature at 400°C, and the gas flow at 500 L/h. The sample solutions subjected to HDX were introduced into the mass spectrometer using a Harvard syringe pump (11 Plus, Harvard Apparatus) at a flow rate of 50 μ L/min.

2. Synthetic procedures:



Scheme S1: Synthetic approach to symmetrically substituted **dBTA (6)**.

4,4'-(((2-((12-Bromododecyl)oxy)propane-1,3-diyl)bis(oxy))bis(methylene))bis(2,2-dimethyl-1,3-dioxolane) (2). A solution of compound **1** (3.05 g, 9.5 mmol, 1 eq) in dioxane (8 mL) was taken in a two necked round bottomed flask under argon atmosphere. Potassium *tert*-butoxide (1.75 g, 15.6 mmol, 1.6 eq) was added to the reaction mixture while cooling it in an ice bath. To the mixture, 1,12-dibromododecane (9.35 g, 28.5 mmol, 3 eq) dissolved in dioxane (6 mL) was added. The reaction mixture was allowed to warm up to room temperature after addition. The progress of the reaction was monitored by TLC and no considerable change in the reaction mixture was observed after 4-5 h. The reaction mixture was diluted with DCM (200 mL) and washed with water. The organic phase was dried over Na_2SO_4 (anhydrous). The organic phase was concentrated under reduced pressure and dried under high vacuum. The crude product was purified by column chromatography to isolate 2.8 g of pure product (yield 52 %). Eluent: 25-60 % EtOAc/Heptane. Unreacted G1-dendron (0.95 g) was also isolated by washing the column with EtOAc.

^1H NMR (400 MHz, CDCl_3) δ = 4.28-4.21 (2H, m), 4.04 (2H, dd, J = 8 and 6.4 Hz), 3.77- 3.38 (15H, m), 1.89-1.81 (2H, m), 1.56-1.51 (2H, m), 1.43-1.26 (28H, m). ^{13}C NMR (101 MHz, CDCl_3) δ = 139.36, 114.22, 109.47, 109.40, 78.86, 78.84, 77.87, 77.36, 74.94, 74.92, 74.79, 74.76, 72.62, 72.60, 72.57, 72.56, 72.09, 72.06, 71.93, 71.86, 71.82, 71.77, 71.75, 71.72, 71.55, 70.86, 70.81, 70.78, 70.75, 67.13, 66.99, 66.96, 66.94, 66.93, 34.17, 33.95, 32.97, 30.22, 29.78, 29.72, 29.69, 29.65, 29.61, 29.56, 29.27, 29.07, 28.90, 28.31, 26.96, 26.91, 26.25, 26.22, 25.57, 25.53.

2-(12-((1,3-Bis((2,2-dimethyl-1,3-dioxolan-4-yl)methoxy)propan-2-yl)oxy)dodecyl)isoindoline-1,3-dione (3). Compound **2** (810 mg, 1.45 mmol, 1 eq) was dissolved in dry DMF (15 mL) in a round bottom flask under argon atmosphere. Potassium phthalimide (598 mg) was added to the solution and the reaction mixture was left stirring at 60 °C for 3-4 h. Complete conversion of the bromide was confirmed by TLC (eluent: 40 % EtOAc/Heptane). The reaction mixture was cooled to room temperature and added water. The compound was extracted into EtOAc (3 x 50 mL) and the combined organic phase was washed further with water and brine solution. The organic phase was dried over Na₂SO₄ (anhydrous) and filtered. The filtrate was concentrated under reduced pressure and dried under high vacuum. The crude product was purified by column chromatography to isolate pure product (867 mg, yield 95%). Eluent: 20-60 % EtOAc/Heptane.

¹H NMR (400 MHz, CD₂Cl₂) δ = 7.82 (dd, 2H, J = 5.6 and 3.2 Hz), 7.72 (dd, 2H, J = 5.6 and 3.2 Hz), 4.24- 4.18 (2H, m), 4.01 (dd, 2H, J = 6.4 and 8.4 Hz), 3.70-3.62 (4H, m), 3.54-3.42 (11H, m), 1.68-1.61 (2H,m), 1.55-1.48 (2H, m), 1.37-1.26 (28H, m). ¹³C NMR (101 MHz, CD₂Cl₂) δ = 168.85, 134.35, 132.82, 123.45, 109.77, 109.71, 78.32, 75.29, 73.78, 73.10, 73.05, 71.96, 71.86, 71.83, 71.81, 71.07, 71.01, 70.97, 70.94, 70.92, 67.27, 67.25, 67.18, 67.16, 64.50, 38.52, 31.16, 30.72, 30.64, 30.18, 30.15, 30.14, 30.12, 30.08, 30.07, 30.02, 29.77, 29.76, 29.11, 27.45, 27.11, 26.68, 26.64, 25.77, 25.74. FT-IR (cm⁻¹): 2985, 2927, 2855, 1773, 1714, 1467, 1438, 1396, 1370, 1255, 1213, 1053, 844, 793, 721, 530. MALDI-TOF-MS: Calculated for C₃₅H₅₅NO₉ M_w= 633.39 g/mol. Observed *m/z* 656.40 g/mol [Na⁺ adduct].

12-((1,3-Bis((2,2-dimethyl-1,3-dioxolan-4-yl)methoxy)propan-2-yl)oxy)dodecan-1-amine (4).

Compound **3** (3.1 g, 4.89 mmol, 1 eq) was dissolved in absolute ethanol (40 mL) in a round bottom flask. Hydrazine hydrate (4 g, 82 mmol, 16 eq) was added to the solution and the reaction mixture was left stirring at 80 °C overnight. After concentrated the reaction mixture under reduced pressure, the solid was dissolved in 1 N NaOH solution. The compound was extracted into CH₂Cl₂ (3 x 70 mL). The combined organic layers were dried over Na₂SO₄ (anhydrous) and filtered. The filtrate was concentrated and the crude product was purified by column chromatography to obtain pure product (2.3 g, yield 93 %). Eluent: DCM- 10% isopropylamine/DCM.

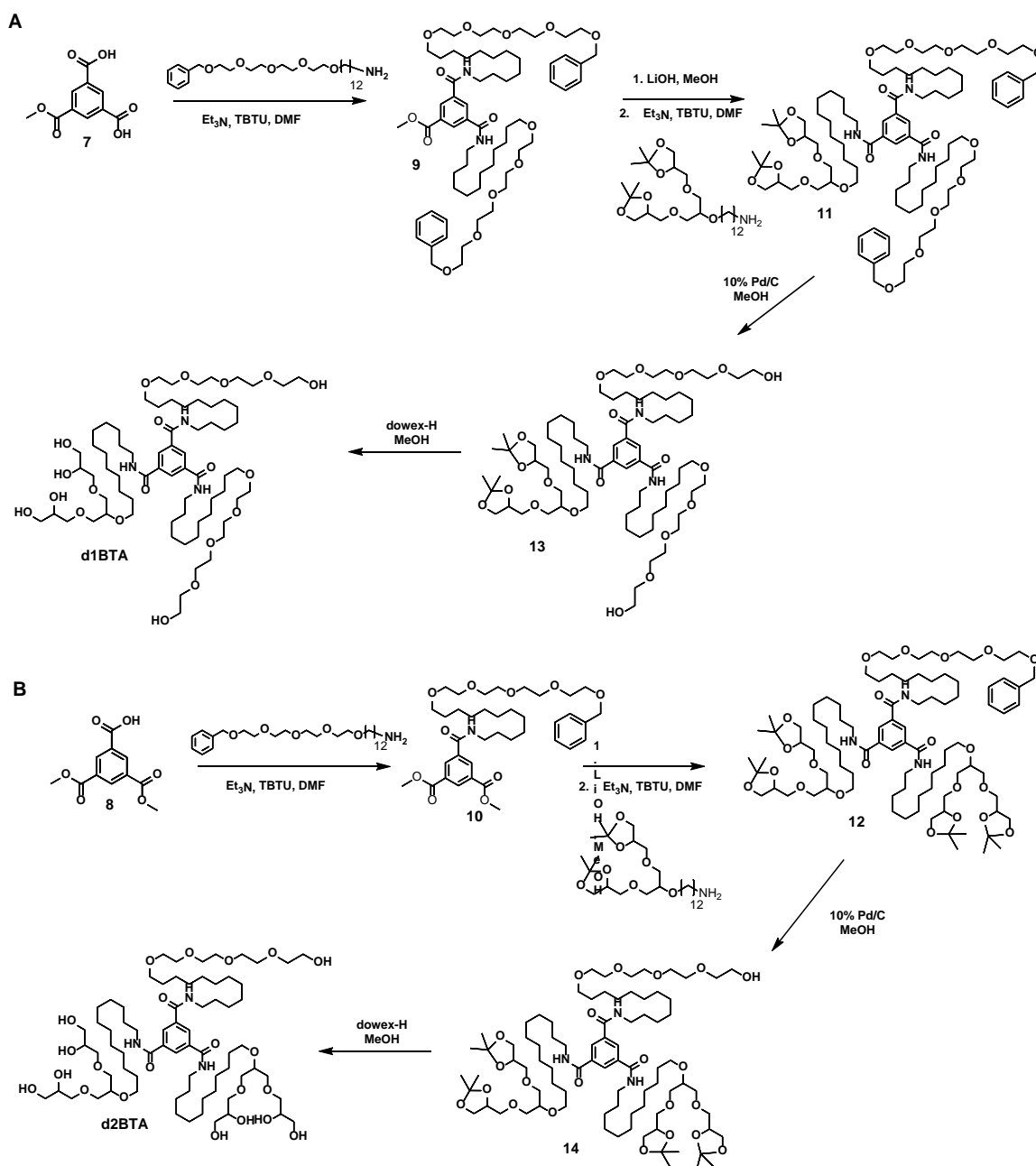
¹H NMR (399 MHz, CD₂Cl₂) δ = 4.24- 4.18 (2H, m), 4.01 (2H, dd, J =8 and 6.4 Hz), 3.70-3.66 (2H, 2d, J = 6.4 and 8 Hz), 3.56-3.42 (11H, m), 2.62 (2H, t, J = 6.8 Hz), 1.56-1.48 (2H, m), 1.42-1.27 (28H, m). ¹³C NMR (100 MHz, CD₂Cl₂) δ = 109.72, 78.33, 75.30, 73.07, 71.98, 71.84, 71.82, 71.02, 70.97, 70.92, 67.27, 67.26, 42.87, 34.64, 30.73, 30.25, 30.21, 30.13, 30.08, 27.49, 27.11, 26.69, 25.78. FT-IR (cm⁻¹): 2986, 2924, 2854, 1456, 1370, 1255, 1213, 1077, 1052, 975, 843, 792, 722, 515. MALDI-TOF-MS: Calculated for C₂₇H₅₃NO₇ M_w= 503.38 g/mol, Observed *m/z* 504.41 [H⁺ adduct].

NI,N3,N5-Tris(12-((1,3-bis((2,2-dimethyl-1,3-dioxolan-4-yl)methoxy)propan-2-yl)oxy)dodecyl)benzene-1,3,5-tricarboxamide (5). Compound **4** (1.2 g, 2.38 mmol, 3.7 eq) was dissolved in dry DCM (10 mL) under argon atmosphere and Et₃N (194 mg, 1.92 mmol, 3 eq) was added. The reaction mixture was cooled in an ice bath and benzene-1,3,5-tricarbonyl trichloride (170 mg, 0.64 mmol, 1 eq) was added dropwise. The reaction mixture was left stirring overnight at room temperature. The progress of the reaction was followed by TLC. The reaction mixture was diluted with DCM and washed with water. The organic phase was dried over Na₂SO₄ (anhydrous), filtered and concentrated under reduced pressure. The crude product was dried and purified by column chromatography to obtain pure product (0.9 g, yield 84%). Eluent: 25-50% EtOAc/DCM.

¹H NMR (400 MHz, acetone-*d*₆) δ = 8.40 (3H, s), 8.01 (3H, t, J = 5.6 Hz), 4.23-4.16 (6H, m), 4.04-3.99 (6H, m), 3.75-3.40 (45H, m), 1.67-1.60 (6H, m), 1.55-1.49 (6H, m), 1.41-1.27 (84H, m). ¹³C NMR (101 MHz, acetone-*d*₆) δ = 166.30, 166.23, 136.51, 136.48, 128.93, 109.54, 109.46, 79.47, 79.46, 78.75, 78.74, 78.71, 75.69, 75.58, 73.11, 73.09, 72.47, 72.42, 72.37, 72.25, 72.23, 72.15, 72.13, 71.93, 71.50, 71.47, 70.82, 70.78, 70.75, 67.59, 67.39, 67.36, 40.61, 40.49, 30.96, 30.51, 30.39, 30.37, 30.35, 30.28, 30.13, 30.09, 29.37, 27.76, 27.19, 27.14, 26.94, 26.92, 25.77, 25.74.

MALDI-TOF-MS: Calculated for C₉₀H₁₅₉N₃O₂₄ M_w= 1666.13 g/mol, Observed *m/z* 1690.14 [Na⁺ adduct].

dBTA (6). Compound **5** was dissolved in methanol (10 mL) and left stirring with dowex-H (2 g) overnight. The progress of the reaction was monitored by NMR. After complete deprotection, the reaction mixture was filtered and dowex was washed with methanol. The filtrate was concentrated and dried. The crude product was purified by reverse phase column chromatography. Eluent: MeOH. ¹H NMR (400 MHz, CD₃OD) δ = 8.37 (3H, s), 3.78-3.38 (57H, m), 1.68-1.53 (12H, m), 1.42-1.31 (48H, m). ¹³C NMR (101 MHz, CD₃OD) δ = 168.63, 136.85, 129.73, 79.90, 79.86, 79.20, 79.17, 79.16, 73.98, 73.97, 73.94, 73.92, 72.96, 72.89, 72.65, 72.44, 72.21, 72.20, 72.18, 72.16, 71.74, 71.71, 71.52, 64.47, 64.42, 64.39, 54.80, 41.23, 31.11, 30.74, 30.71, 30.69, 30.59, 30.57, 30.47, 28.11, 27.23, 27.19. MALDI-TOF-MS: Calculated for C₇₂H₁₃₅N₃O₂₄ M_w= 1425.94 g/mol, Observed *m/z* 1448.95 g/mol [Na⁺ adduct].



Scheme S2: Synthetic approach to desymmetrised A) **d1BTA** and B) **d2BTA**.

Compound 9. A solution of compound **7** (301 mg, 1.34 mmol, 1 eq) in DMF (6 mL) was taken in a round bottom flask under argon atmosphere. Triethylamine (1 mL, 7.11 mmol, 5.3 eq) was added to the reaction mixture. The reaction mixture was cooled down by an ice bath. TBTU (1.25 g, 3.89 mmol, 2.9 eq) and 1-phenyl-2,5,8,11,14-pentaoxahexacosan-26-amine (1.25 g, 2.67 mmol, 2 eq) were added to the reaction mixture. The reaction mixture was allowed to warm up to room temperature by removing the ice bath and allowed to stir at room temperature overnight. Progress of the reaction was monitored by TLC. After complete conversion of the starting material, the reaction mixture was quenched by adding water and the compound was extracted into EtOAc (2 x 60 mL). The combined organic phase was washed further with water and dried over Na_2SO_4 (anhydrous). The filtrate was

concentrated, dried and purified by column chromatography to obtain pure product (1.1 g, yield 73%).

Eluent: 20-80% EtOAc/DCM.

^1H NMR (399 MHz, CDCl_3) δ = 8.55 (2H, d), 8.43 (1H, t), 7.34-7.24 (10H, m), 6.64 (2H, t), 4.55 (4H, s), 3.95 (3H, s), 3.69-3.61 (28H, m), 3.57-3.54 (4H, m), 3.47-3.41 (8H, m), 1.65-1.52 (8H, m), 1.40-1.26 (32H, m). ^{13}C NMR (100 MHz, CDCl_3) δ = 165.92, 165.88, 165.70, 138.31, 135.59, 131.09, 130.86, 130.69, 129.67, 128.44, 128.37, 127.84, 127.69, 77.36, 73.34, 71.63, 70.75, 70.74, 70.72, 70.70, 70.14, 69.53, 53.55, 52.66, 40.50, 38.71, 29.71, 29.69, 29.63, 29.62, 29.59, 29.54, 29.42, 29.40, 27.11, 26.19, 26.16. FT-IR (cm^{-1}): 3346, 2924, 2854, 1728, 1663, 1539, 1453, 1350, 1254, 1198, 1102, 741, 698. MALDI-TOF-MS: Calculated for $\text{C}_{64}\text{H}_{102}\text{N}_2\text{O}_{14}$ M_w = 1122.73 g/mol, Observed m/z 1145.73 [Na^+ adduct].

Compound 10. To a solution of compound **8** (304 mg, 1.27 mmol, 1 eq) in DMF (6 mL), triethylamine (0.5 mL, 3.56 mmol, 2.8 eq) was added and the reaction mixture was cooled in an ice bath. TBTU (600 mg, 1.86 mmol, 1.47 eq) and 1-phenyl-2,5,8,11,14-pentaoxahexacosan-26-amine (650 mg, 1.38 mmol, 1.1 eq) were added to the above reaction mixture and the reaction mixture was allowed stir at room temperature overnight. The progress of the reaction was monitored by TLC. The reaction was quenched by adding water and the compound was extracted into EtOAc (3 x 60 mL). The combined organic phase was washed with water twice and dried over anhyd. Na_2SO_4 . The filtrate was concentrated, dried and purified by column chromatography to obtain pure product (580 mg, yield 66 %).

^1H NMR (400 MHz, CDCl_3) δ = 8.76 (1H, t, J = 1.6 Hz), 8.59 (2H, d, J = 1.6 Hz), 7.34-7.24 (5H, m), 6.41 (1H, t, J = 5.6 Hz), 4.55 (2H, s), 3.95 (6H, s), 3.68-3.60 (14H, m), 3.57-3.54 (2H, m), 3.48-3.40 (4H, m), 1.66-1.51 (4H, m), 1.37-1.23 (16H, m). ^{13}C NMR (101 MHz, CDCl_3) δ = 165.68, 165.51, 138.36, 135.80, 133.11, 132.16, 131.21, 128.44, 127.83, 127.67, 73.34, 71.63, 70.75, 70.73, 70.71, 70.15, 69.54, 68.07, 64.46, 60.49, 53.55, 52.71, 40.52, 30.74, 29.74, 29.70, 29.66, 29.62, 29.58, 29.42, 27.11, 26.19, 25.72, 21.16, 19.23, 14.31, 13.81. FT-IR (cm^{-1}): 3332, 2924, 2854, 1728, 1645, 1543, 1440, 1277, 1244, 1105, 1000, 742. MALDI-TOF-MS: Calculated for $\text{C}_{38}\text{H}_{57}\text{NO}_{10}$ M_w = 687.40 g/mol, Observed m/z 710.40 [Na^+ adduct]

Compound 11. A solution of compound **9** (1 g, 0.89 mmol, 1 eq) in MeOH (5 mL) was taken in a round bottom flask. LiOH (100 mg, 4.18 mmol, 4.7 eq) and a few drops of water were added to the reaction mixture and allowed to stir for 6-8 h at room temperature. The completion of reaction was confirmed by TLC and the reaction mixture was concentrated under reduced vacuum. 1N HCl was added to the reaction mixture and compound was extracted into EtOAc. The organic phase was dried

over Na₂SO₄ (anhydrous). The filtrate was filtered, concentrated and dried to obtain crude product. The crude product was directly used for the next step.

¹H NMR (400 MHz, CD₃OD) δ = 8.59 (2H, d), 8.47 (1H, t), 7.35-7.23 (10H, m), 4.53 (4H, br s), 3.67-3.58 (28H, m), 3.55-3.52 (4H, m), 3.45-3.37 (8H, m), 1.66-1.49 (8H, m), 1.36-1.28 (32H, m). ¹³C NMR (101 MHz, CD₃OD) δ = 175.13, 172.93, 171.69, 168.35, 168.06, 167.91, 139.63, 138.75, 136.88, 136.85, 133.08, 132.99, 131.96, 131.32, 130.94, 130.28, 129.34, 128.87, 128.81, 128.64, 74.13, 72.35, 71.60, 71.58, 71.55, 71.15, 70.64, 61.51, 41.21, 30.72, 30.68, 30.66, 30.57, 30.43, 30.38, 28.08, 27.20, 20.86, 20.74, 14.47.

The formed acid was dissolved in DMF (5 mL) and triethylamine (0.3 mL, 2.13 mmol, 2.4 eq) was added. The reaction mixture was cooled in an ice bath. TBTU (500 mg, 1.56 mmol, 1.75 eq) and compound **4** (510 mg, 1.01 mmol, 1.34 eq) were added. The reaction mixture was left stirring at room temperature overnight. The conversion was confirmed by TLC (eluent 50% EtOAc/DCM). The reaction mixture was quenched by adding water and the compound was extracted into EtOAc (3 x 20 mL). The combined organic layers were washed with water and dried over Na₂SO₄ (anhydrous). After filtration, the filtrate was concentrated and purified by column chromatography to obtain pure product **11** (1.02 g, yield 72 %). Eluent: 0-10% isopropanol/DCM.

¹H NMR (399 MHz, CD₂Cl₂) δ = 8.33 (3H, s), 7.35-7.24 (10H, m), 6.88- 6.70 (3H, m), 4.52-4.51 (4H, m/2S), 4.23-4.19 (3H, m), 4.03-3.99 (3H, m), 3.70-3.37 (61H, m), 1.61-1.50 (12H, m), 1.37-1.27 (60H, m). ¹³C NMR (100 MHz, CD₂Cl₂) δ = 166.22, 166.18, 139.06, 136.13, 136.01, 128.81, 128.51, 128.25, 128.03, 127.94, 109.71, 78.31, 75.29, 73.64, 73.05, 71.95, 71.92, 71.81, 71.79, 71.13, 71.11, 71.09, 71.07, 71.01, 70.96, 70.91, 70.61, 70.20, 67.25, 64.66, 40.82, 40.80, 40.11, 30.72, 30.28, 30.24, 30.21, 30.19, 30.16, 30.14, 30.10, 30.06, 30.04, 29.99, 29.94, 29.91, 29.89, 29.84, 27.63, 27.61, 27.54, 27.48, 27.11, 26.68, 26.66, 25.77, 25.73, 23.57. FT-IR (cm⁻¹): 3340, 2925, 2855, 1644, 1536, 1455, 1370, 1259, 1214, 1107, 845, 745, 699. MALDI-TOF-MS: Calculated for C₉₀H₁₅₁N₃O₂₀ M_w= 1594.09 g/mol, Observed *m/z* 1617.08 (Na⁺ adduct).

Compound 12. Compound **10** (340 mg, 0.494 mmol, 1 eq) was dissolved in a mixture of methanol (4 mL) and isopropanol (2 mL). To the above solution, LiOH (80 mg, 3.34 mmol, 6.76 eq) and a few drops of water were added. The reaction mixture was left stirring at room temperature overnight. The reaction mixture was concentrated and acidified with 1 N HCl. The compound was extracted into CH₂Cl₂ (3 x 30 mL). The combined organic layers were dried over Na₂SO₄ (anhydrous) and filtered. The filtrate was concentrated and dried to obtain the crude product that was directly used for the next step.

¹H NMR (400 MHz, CD₃OD) δ = 8.76 (1H, t, J = 1.6Hz), 8.67 (2H, d, J = 1.6Hz), 7.35-7.24 (5H, m), 4.54 (2H, s), 3.68-3.59 (14H, m), 3.56-3.53 (2H, m), 3.45-3.35 (4H, m), 1.68-1.61 (2H, m), 1.57-

1.50 (2H, m), 1.42-1.22 (16H, m). ^{13}C NMR (101 MHz, CD_3OD) δ = 172.96, 168.24, 168.01, 139.63, 136.92, 134.21, 133.38, 133.10, 129.34, 128.88, 128.65, 74.14, 72.35, 71.60, 71.58, 71.55, 71.15, 70.64, 61.52, 54.80, 41.20, 30.71, 30.66, 30.64, 30.55, 30.40, 30.36, 28.07, 27.19, 20.86, 14.46.

A solution of above diacid (0.49 mmol) in DMF (5 mL) was taken in round bottom flask. Triethylamine and compound **4** were added to the reaction mixture. The reaction mixture was cooled with an ice bath. Finally, TBTU was added and the reaction mixture was left stirring at room temperature overnight. The reaction mixture was quenched by the addition of water and the compound was extracted into EtOAc (3 x 50 mL). The combined organic layers were washed with water and brine solution, and finally dried over Na_2SO_4 (anhydrous). After filtration, the filtrate was concentrated and purified by column chromatography to obtain pure compound **12** (750 mg, yield 93%). Eluent: 0-10% isopropanol/DCM)

^1H NMR (399 MHz, CD_2Cl_2) δ = 8.32 (3H, s), 7.35-7.24 (5H, m), 6.83-6.79 (2H, m), 6.50 (1H, t), 4.51 (2H, s), 4.24-4.18 (6H, m), 4.03-3.94 (7H, m), 3.70-3.37 (45H, m), 1.62-1.50 (12H, m), 1.37-1.27 (72H, m). ^{13}C NMR (100 MHz, CD_2Cl_2) δ = 166.17, 162.25, 139.07, 136.05, 128.81, 128.47, 128.25, 128.03, 109.71, 78.31, 75.29, 73.64, 73.05, 71.95, 71.91, 71.81, 71.79, 71.13, 71.11, 71.09, 71.01, 70.96, 70.91, 70.61, 70.20, 67.25, 67.23, 64.67, 46.19, 40.83, 40.81, 40.34, 30.72, 30.39, 30.24, 30.20, 30.18, 30.15, 30.13, 30.09, 30.07, 30.05, 30.03, 29.98, 29.93, 29.82, 29.72, 27.62, 27.52, 27.26, 27.11, 26.68, 26.65, 25.77, 25.72. FT-IR (cm^{-1}): 3334, 2985, 2925, 2854, 1662, 1536, 1456, 1370, 1258, 1213, 1077, 1052, 843, 792, 746, 699, 517. MALDI-TOF-MS: Calculated for $\text{C}_{90}\text{H}_{155}\text{N}_3\text{O}_{22}$ $M_w=1630.11$ g/mol, Observed m/z 1653.13 [Na^+ adduct]

Compound 13. A solution of compound **11** (850 mg, 0.533 mmol) in methanol (50 mL) was taken in a Parr reactor bottle and N_2 was bubbled through the solution for 5 min. To the above solution 10% Pd/C (150 mg, 0.14 mmol) was added and the reaction mixture was left shaking under 60 psi H_2 atmosphere for 4 h. After completion of the reaction, nitrogen was bubbled through the reaction mixture for 10 mins and the reaction mixture was filtered through a sintered funnel with a Celite bed. The Celite bed was further washed with methanol and the combined methanolic phase was concentrated under reduced pressure and dried under vacuum. The crude product was purified by column chromatography to obtain pure product **13** (600 mg, yield 79%). Eluent: 0-10% isopropanol/DCM.

^1H NMR (400 MHz, CD_3OD) δ = 8.37 (3H, s), 4.27-4.21 (2H, m), 4.04 (2H, dd, J = 8 and 6.4 Hz), 3.93 (1H, m), 3.74-3.38 (54H, m), 1.66-1.51 (12H, m), 1.42-1.31 (60H, m). ^{13}C NMR (101 MHz, CD_3OD) δ = 168.56, 136.84, 129.74, 110.45, 79.20, 76.15, 73.68, 73.41, 73.39, 72.41, 72.37, 72.34, 71.61, 71.56, 71.55, 71.48, 71.46, 71.44, 71.41, 71.16, 67.60, 64.73, 62.23, 54.81, 41.22, 31.15, 30.77, 30.74, 30.71, 30.69, 30.59, 30.49, 30.47, 28.12, 28.10, 27.24, 27.22, 27.11, 25.71, 25.26. FT-IR (cm^{-1}

¹):3332, 2923, 2854, 1645, 1537, 1456, 1370, 1287, 1259, 1214, 1103, 934, 843, 707, 515. MALDI-TOF-MS: Calculated for C₇₆H₁₃₉N₃O₂₀ M_w= 1413.99 g/mol, Observed *m/z* 1436.98 [Na⁺ adduct]

Compound 14. A methanolic solution (50 mL) of compound **12** (700 mg, 0.429 mmol, 1 eq) was taken in a Parr reactor bottle and N₂ was bubbled through the solution for 5 min. Then, 10% Pd/C (150 mg, 0.141 mmol, 0.33 eq) was added to the above solution and the reaction vessel was left shaking under 60 psi H₂ pressure for 6 h. Completion of the reaction was confirmed by TLC (5% isopropanol/CDM). Nitrogen was bubbled through the reaction mixture for 10 min and the reaction mixture was filtered through a bed of Celite using a sintered funnel. The Celite was further washed with methanol (50 mL). The combined methanolic phase was concentrated and dried. The crude product was purified by column chromatography to obtain pure product (480 mg, yield 73 %). Eluent: 0-15% isopropanol/DCM.

¹H NMR (399 MHz, CD₂Cl₂) δ = 8.31 (3H, s), 6.95-6.91 (3H, m), 4.22-4.17 (4H, m), 4.01 (4H, dd, J= 8 and 6.4 Hz), 3.69-3.36 (50H, m), 1.62-1.48 (12H, m), 1.37-1.25 (72H, m). ¹³C NMR (100 MHz, CD₂Cl₂) δ = 166.30, 136.01, 135.99, 128.53, 109.71, 78.31, 75.28, 73.09, 73.05, 71.93, 71.80, 71.78, 71.13, 71.07, 71.04, 71.00, 70.95, 70.90, 70.84, 70.59, 67.24, 67.23, 62.12, 40.84, 40.81, 30.71, 30.21, 30.18, 30.16, 30.10, 30.07, 30.05, 30.02, 30.00, 29.94, 29.80, 27.63, 27.51, 27.10, 26.68, 26.62, 25.77. FT-IR (cm⁻¹): 3250, 2924, 2854, 1642, 1557, 1456, 1370, 1257, 1213, 1105, 844, 691, 515. MALDI-TOF-MS: Calculated for C₈₃H₁₄₉N₃O₂₂ M_w= 1540.06, Observed *m/z* 1563.07 (Na⁺ adduct)

d1BTA. To a solution of compound **13** (324 mg, 0.229 mmol) in methanol (5 mL), 1 g of Dowex-H was added and the reaction mixture was kept stirring at room temperature overnight. The completion of the reaction was confirmed by reverse phase TLC. The reaction mixture was filtered and the Dowex was washed with methanol (50 mL). The filtrate was concentrated and purified by reverse phase column chromatography to obtain pure product (213 mg, yield 70%). Eluent: methanol

¹H NMR (399 MHz, CD₃OD) δ = 8.38 (3H, s), 3.78-3.36 (59H, m), 1.65-1.53(12H, m), 1.41-1.30 (48H, m). ¹³C NMR (100 MHz, CD₃OD) δ = 168.41, 136.70, 129.74, 79.83, 79.79, 79.12, 79.10, 79.08, 73.94, 73.92, 73.89, 73.87, 73.60, 72.91, 72.84, 72.59, 72.44, 72.41, 72.37, 72.32, 72.18, 72.14, 72.12, 72.10, 71.70, 71.67, 71.50, 71.46, 71.45, 71.44, 71.30, 71.06, 64.44, 64.42, 64.41, 64.38, 64.34, 62.13, 41.22, 31.08, 30.72, 30.70, 30.68, 30.67, 30.61, 30.57, 30.55, 30.46, 30.45, 28.10, 28.08, 27.19, 27.16, 27.15. MALDI-TOF-MS: Calculated for C₇₀H₁₃₁N₃O₂₀ M_w = 1334.82 g/mol. Observed *m/z* 1372.91 [K⁺ adduct].

d2BTA. A solution of compound **14** (330 mg, 0.214 mmol, 1 eq) was dissolved in methanol (6 mL) and stirred with 1 g of Dowex-H overnight. Completion of the reaction was confirmed by NMR. The

reaction mixture was filtered through a whatman filter paper and dowex was further washed with methanol. The filtrate was concentrated and purified by reverse phase column chromatography to obtain pure product (230 mg, Yield 78%). Eluent: methanol.

^1H NMR (399 MHz, CD_3OD) δ = 8.38 (3H, s), 3.76-3.37 (58H, m), 1.66-1.51 (12H, m), 1.40-1.30 (48H, m). ^{13}C NMR (100 MHz, CD_3OD) δ = 168.40, 136.72, 129.75, 79.85, 79.81, 79.13, 79.11, 79.10, 73.95, 73.93, 73.91, 73.89, 73.63, 72.93, 72.86, 72.60, 72.44, 72.39, 72.38, 72.32, 72.15, 72.14, 72.12, 71.72, 71.69, 71.53, 71.49, 71.47, 71.45, 71.40, 71.33, 71.09, 64.45, 64.43, 64.39, 64.35, 62.16, 62.14, 41.21, 31.09, 30.72, 30.69, 30.68, 30.63, 30.59, 30.57, 30.48, 30.46, 28.11, 28.10, 27.21, 27.18, 27.17. MALDI-TOF-MS: Calculated for $\text{C}_{71}\text{H}_{133}\text{N}_3\text{O}_{22}$ $M_w = 1379.94$. Observed m/z 1418.91 [K^+ adduct].

3. Supplementary Figures

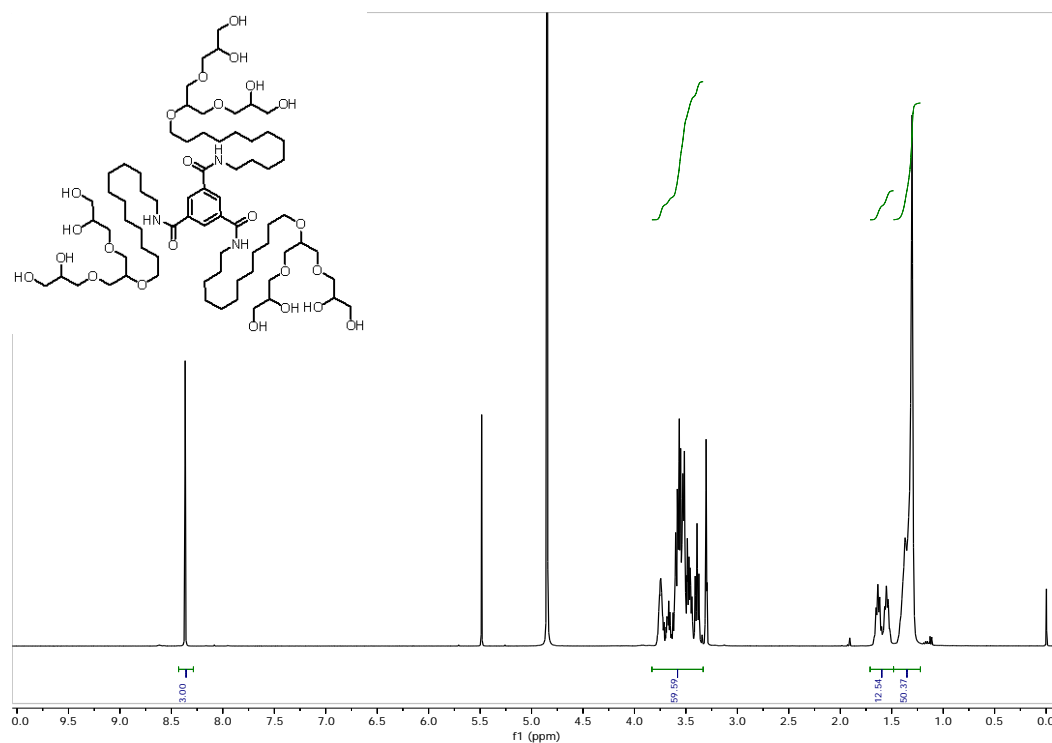


Figure S1: ¹H-NMR of dBTA in CD₃OD

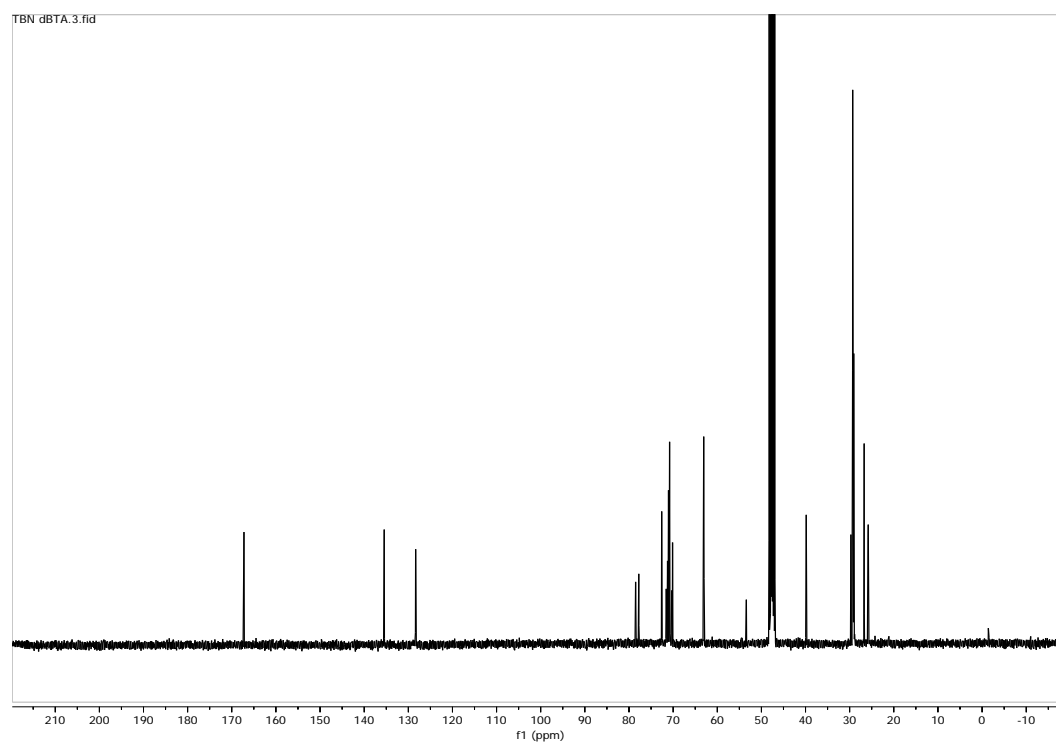


Figure S2: ¹³C-NMR of dBTA in CD₃OD

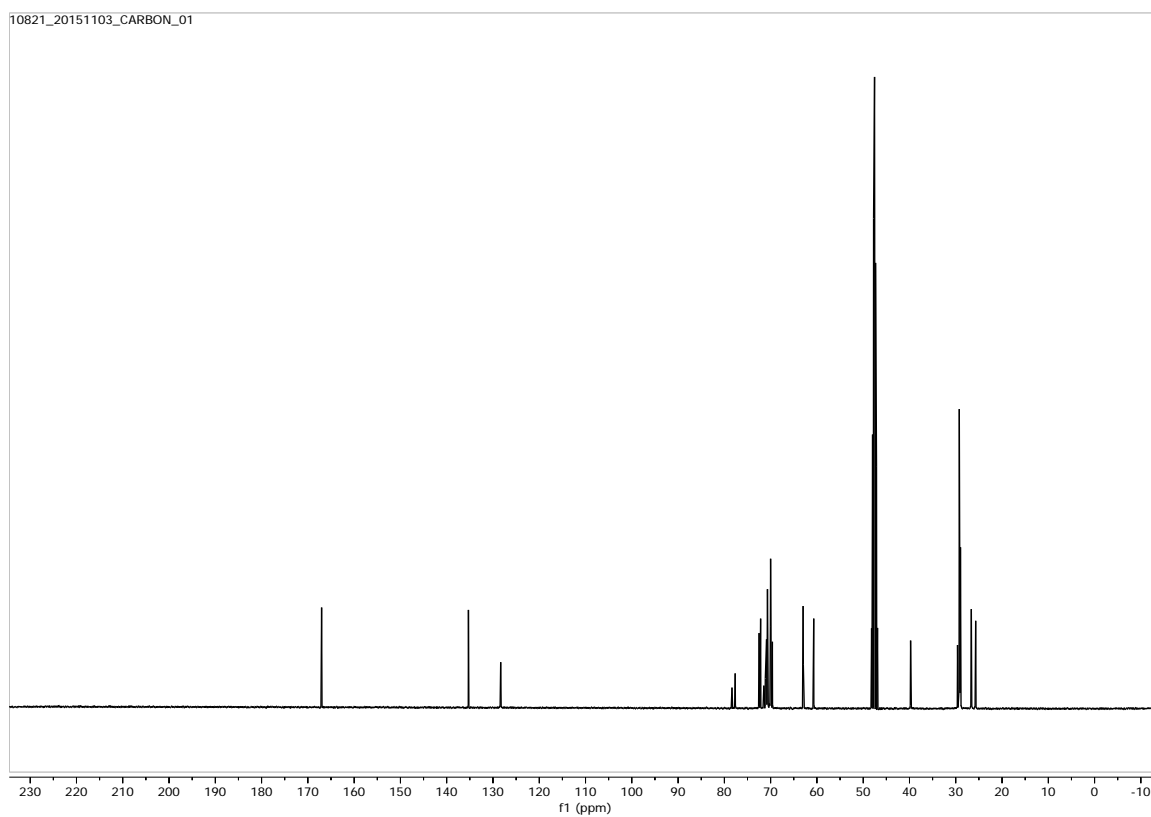


Figure S5: ^{13}C -NMR of **d1BTA** in CD_3OD

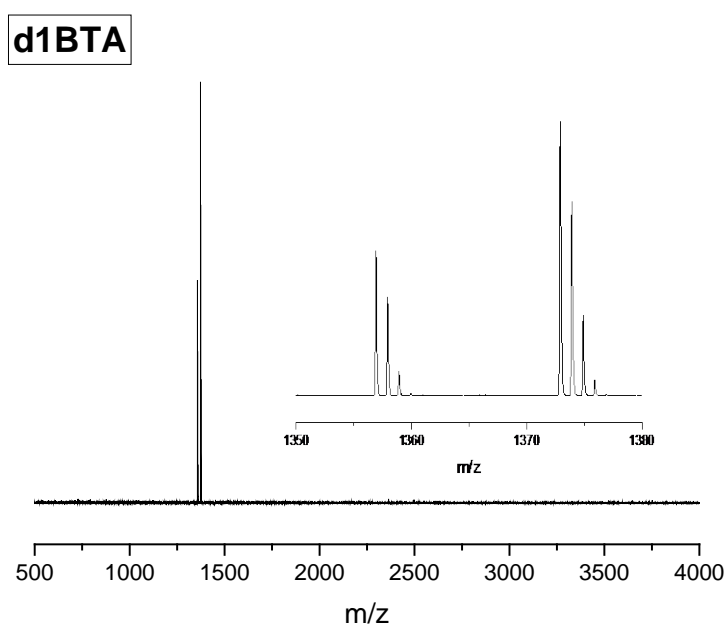


Figure S6: Maldi-ToF MS of **d1BTA**

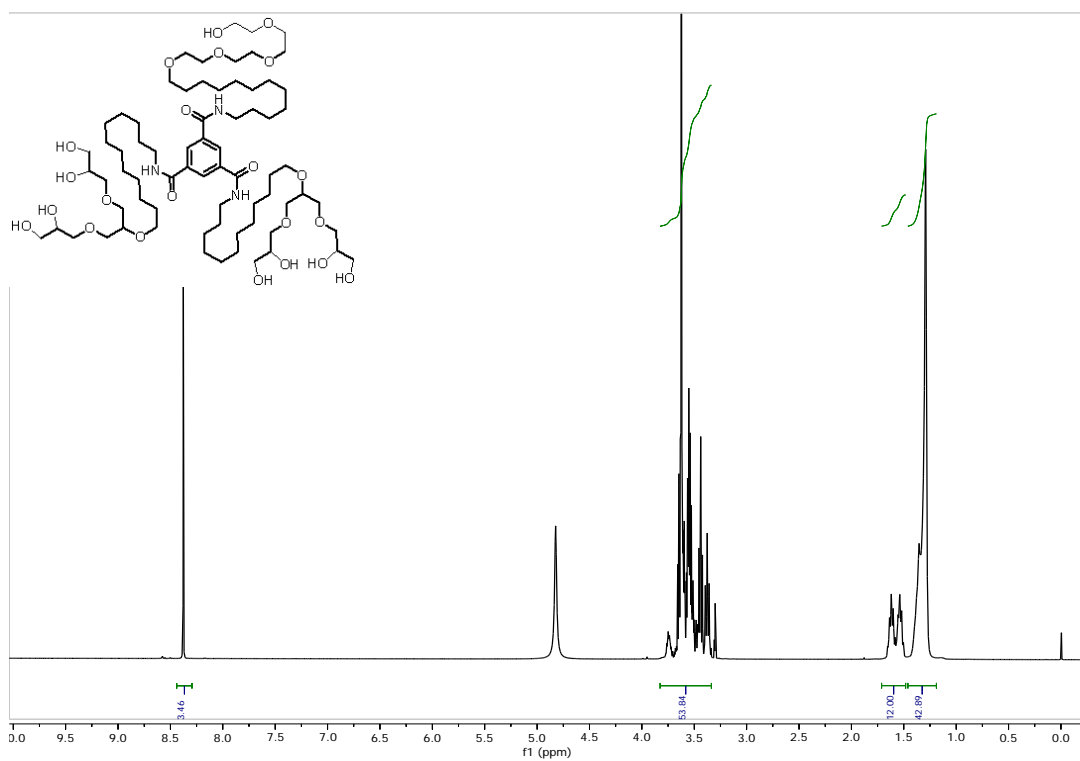


Figure S7: $^1\text{H-NMR}$ of d2BTA in CD_3OD

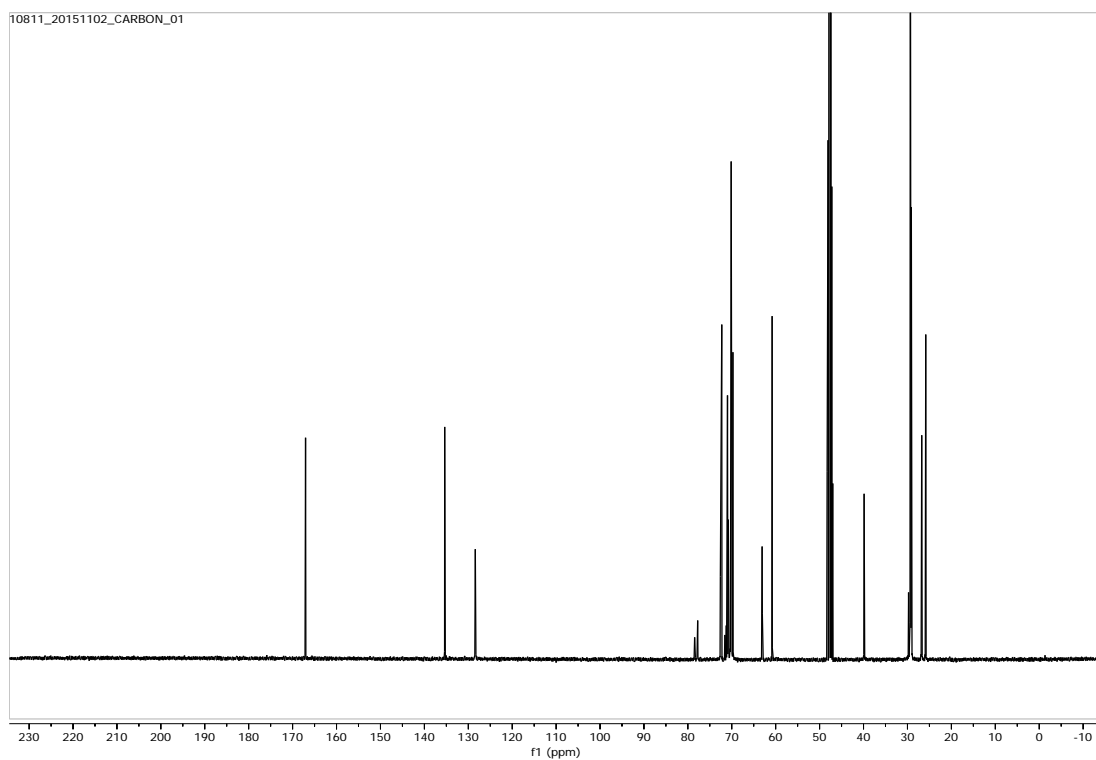


Figure S8: $^{13}\text{C-NMR}$ of d2BTA in CD_3OD

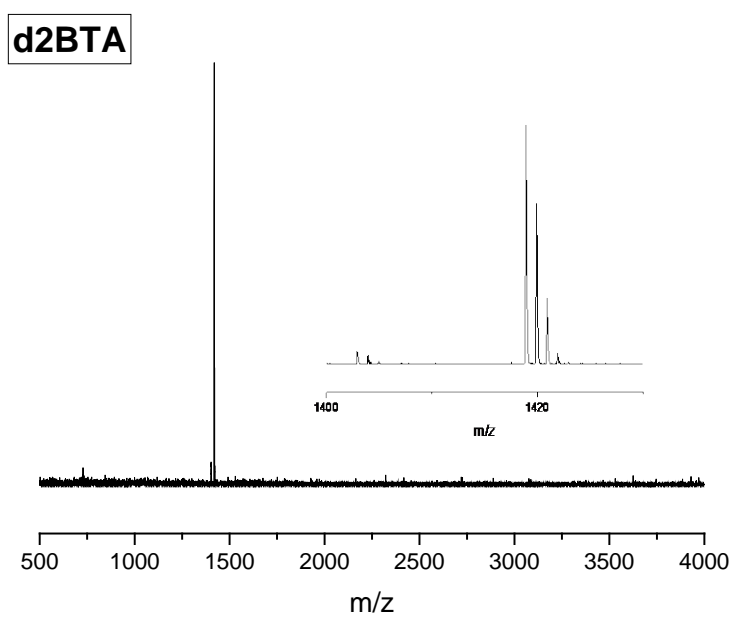


Figure S9: Maldi-ToF MS of **d2BTA**

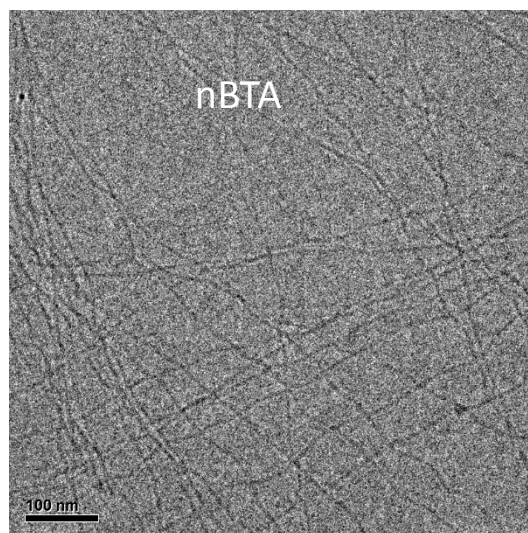


Figure S10: CryoTEM image of **nBTA**; $c_{\text{BTA}} = 582 \mu\text{M}$, scale bar is 100 nm

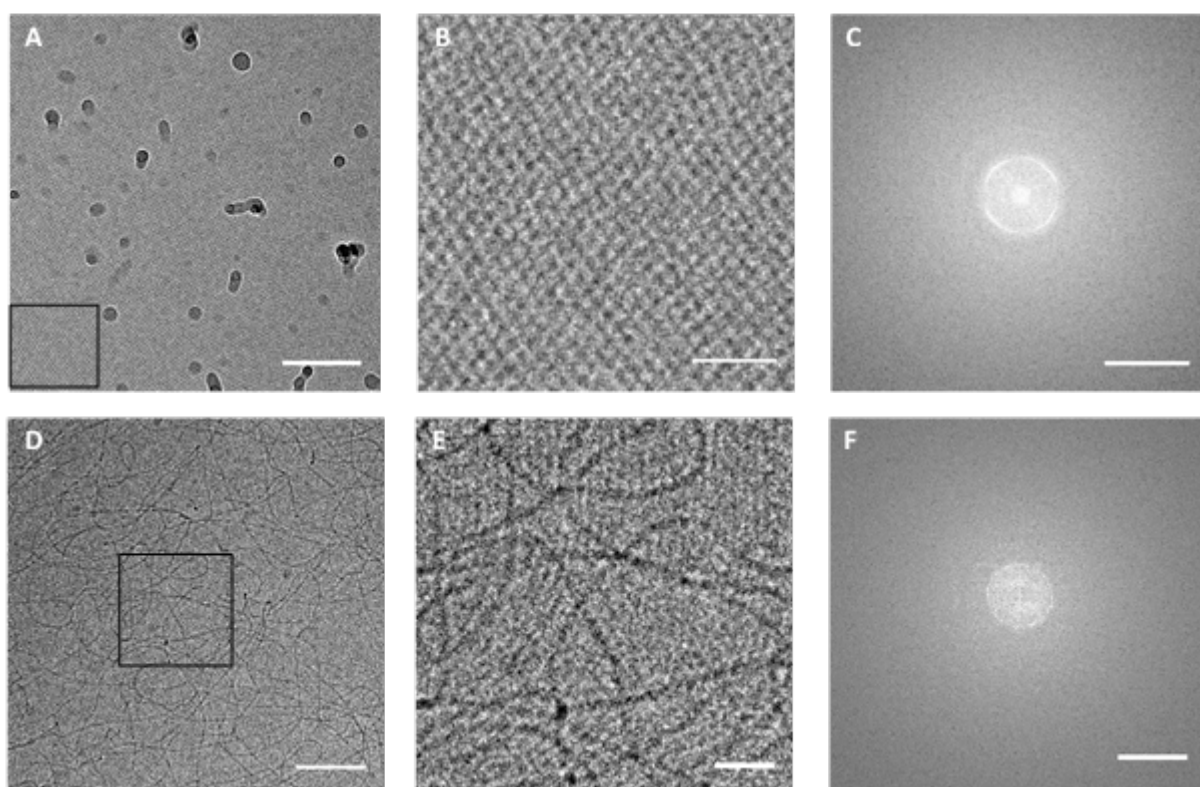


Figure S11: CryoTEM images A) of **dBTA** ($c_{\text{BTA}} = 1\text{mM}$), scale bar = 100 nm, larger dark spots are surface contamination; B) close-up of marked area, scale bar = 25 nm; C) FFT of A, scale bar 500 $1/\mu\text{m}$; D) of a 1:2 mixture of **nBTA:dBTA** ($c_{\text{BTA}} = 1\text{mM}$), scale bar = 100 nm; E) close-up of marked area, scale bar = 25 nm; F) FFT of D, scale bar 500 $1/\mu\text{m}$.

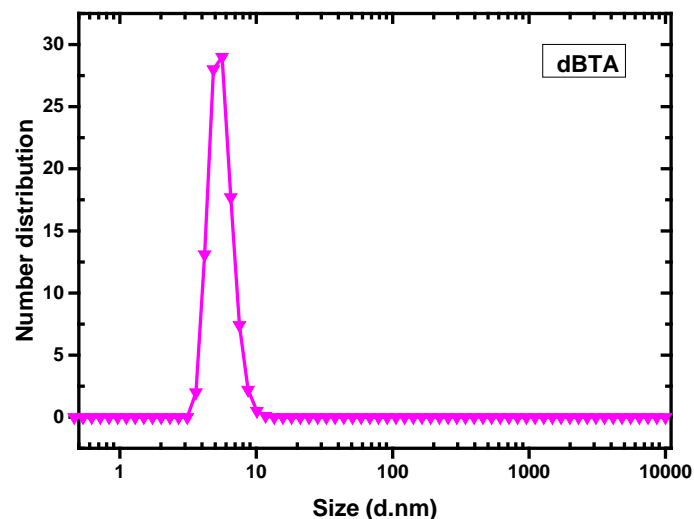


Figure S12: Dynamic light scattering measurement of **dBTA** in H₂O ($c = 1\%$ w/w)

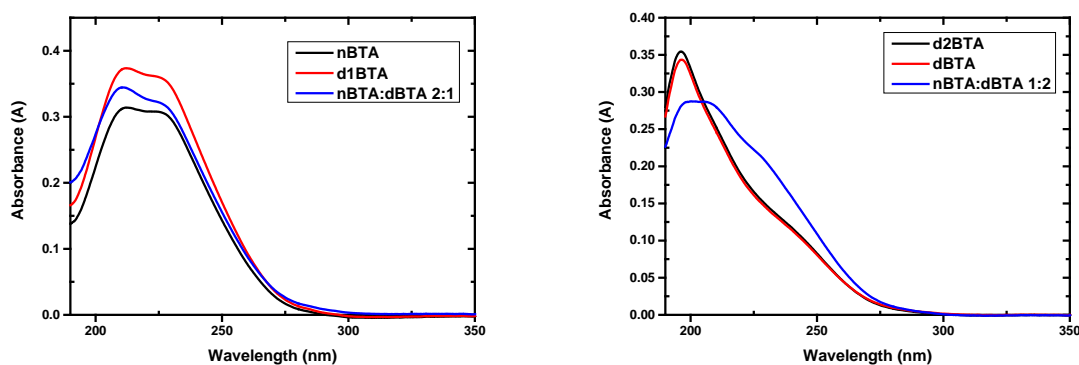


Figure S13: UV-vis spectra of **d1BTA** and **d2BTA** in water at room temperature. Samples were measured 20 h after heating @80 °C for 2 h at $c_{\text{BTA}} = 100\ \mu\text{M}$ (path length = 1 mm). The spectra of **nBTA** and **dBTA** homopolymers as well as mixtures of **nBTA** and **dBTA** are added for comparison.

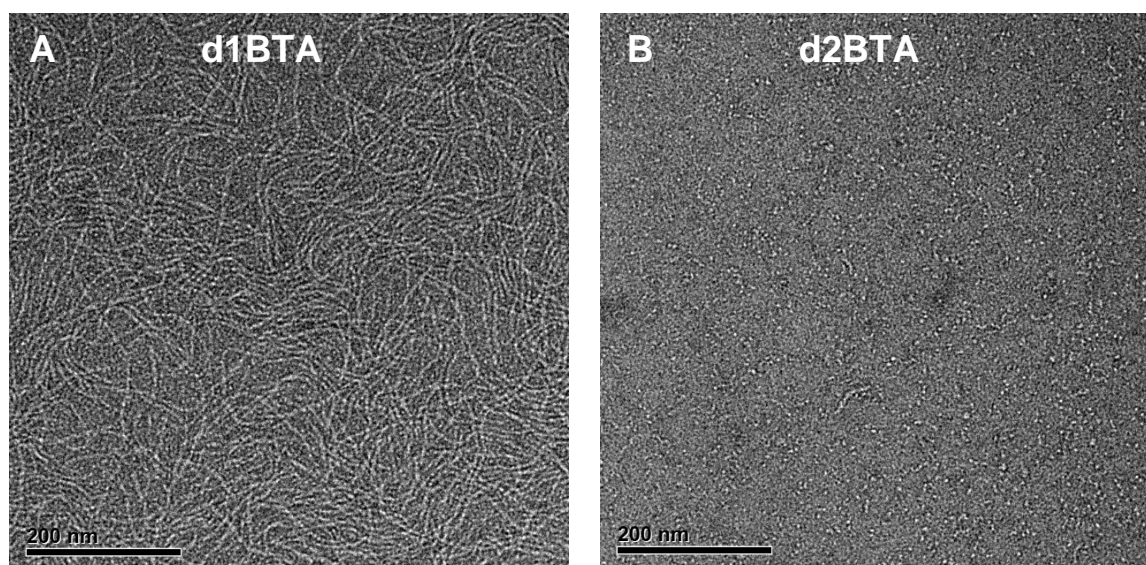


Figure S14: TEM images of **d1BTA** and **d2BTA**; $c_{\text{BTA}} = 200 \mu\text{M}$.

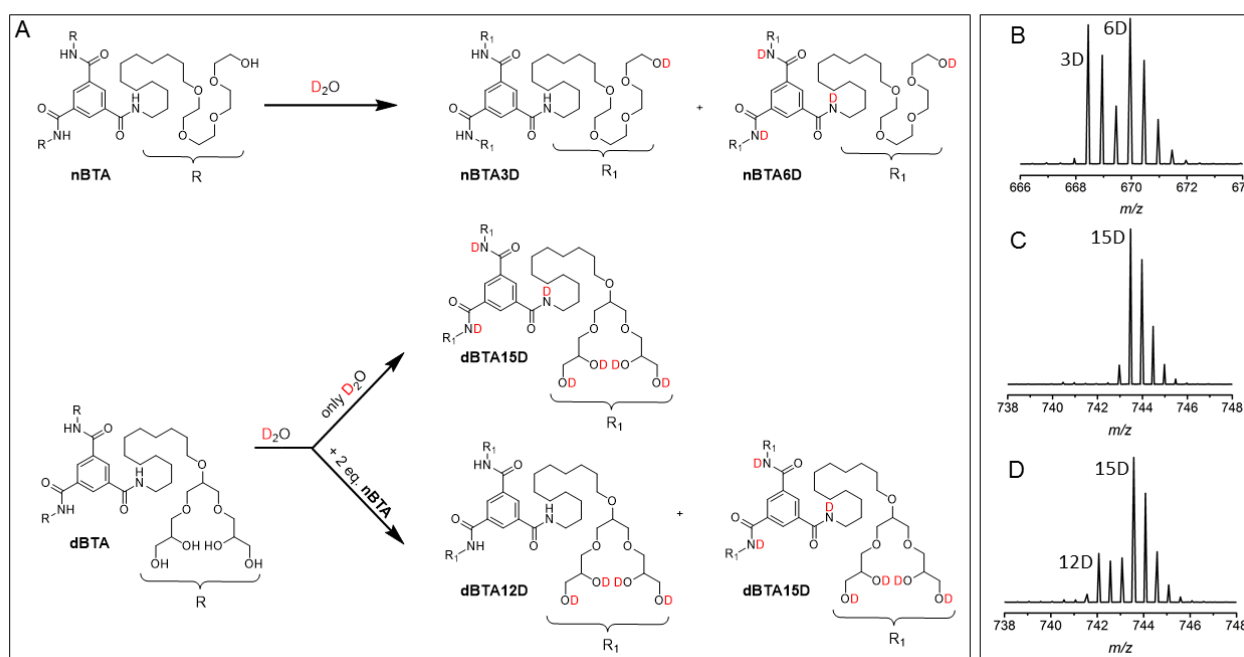


Figure S15. A) HDX of **nBTA** or **dBTA** after dilution in D_2O in which either only OH is replaced by OD or also NH is replaced to ND. B) ESI-MS of **nBTA** taken after 1 h shows two isotopic distributions corresponding to **nBTA3D** and **nBTA6D**. C) ESI-MS of **dBTA** taken after 3 min shows only one isotopic distribution corresponding to **dBTA15D**. D) ESI-MS of **dBTA** of a 2:1 mixture of **nBTA** and **dBTA** taken after 1 h shows two isotopic distributions corresponding to **dBTA12D** and **dBTA15D**.

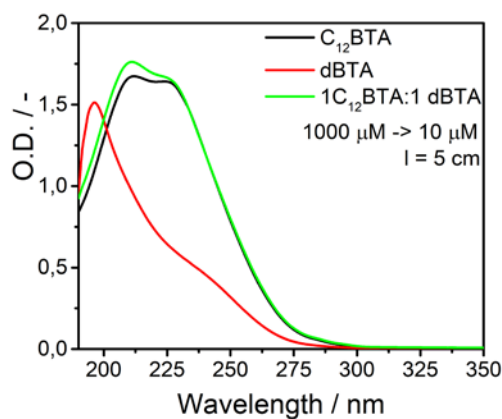


Figure S16: UV-Vis measurements of **nBTA**, **dBTA** and a 1/1 mixture of **nBTA**/**dBTA** in H₂O at $c_{\text{BTA}} = 10 \mu\text{M}$. Also at this low concentration both **nBTA** as well as the 1/1 mixture of **nBTA**/**dBTA** show the same UV signature as at the higher concentrations, indicating that the nature of supramolecular aggregates remains intact.

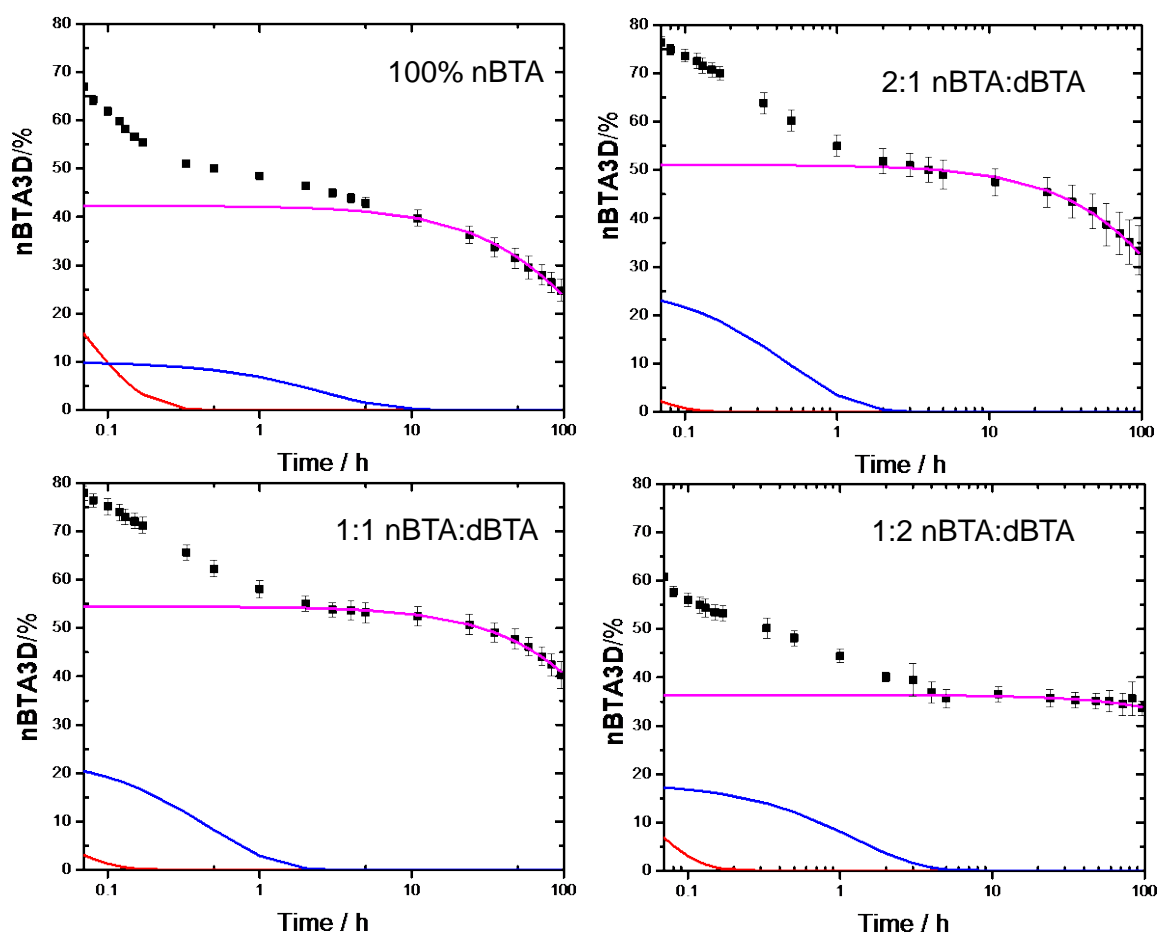


Figure S17: Results of fitting the tri-exponential model (lines) to the time-dependent HDX-MS decay data of **nBTA3D** (markers). The lines represent the contributions of each exponential term in the model, corresponding to the initial (red), the fast (blue) and the slow (pink) decays.

Table S1. Rate constants k and relative contributions of HDX for different exchanging parts of **nBTA** and different polymer compositions.

System	k_{initial} (h^{-1})	k_{fast} (h^{-1})	k_{slow} (h^{-1})	Initial (%)	Fast (%)	Slow (%)
nBTA	1.58×10^1	0.38	5.87×10^{-3}	47.54	10.03	42.35
2:1 nBTA:dBTA	3.37×10^1	2.04	4.58×10^{-3}	22.39	26.52	51.09
1:1 nBTA:dBTA	2.82×10^1	2.11	2.96×10^{-3}	21.89	23.64	54.48
1:2 nBTA:dBTA	2.70×10^1	0.81	7.49×10^{-4}	45.36	18.23	36.41

Table S2. Rate constants k and relative contributions of HDX for different exchanging parts of **dBTA** and different polymer compositions.

System	k_{initial} (h^{-1})	k_{fast} (h^{-1})	k_{slow} (h^{-1})	Initial (%)	Fast (%)	Slow (%)
2:1 nBTA:dBTA	3.52×10^1	4.32	4.45×10^{-3}	56.68	22.90	20.41
1:1 nBTA:dBTA	3.09×10^1	5.00	2.72×10^{-3}	59.86	20.87	19.27
1:2 nBTA:dBTA	3.64×10^1	1.59	2.22×10^{-14}	80.25	11.12	8.64

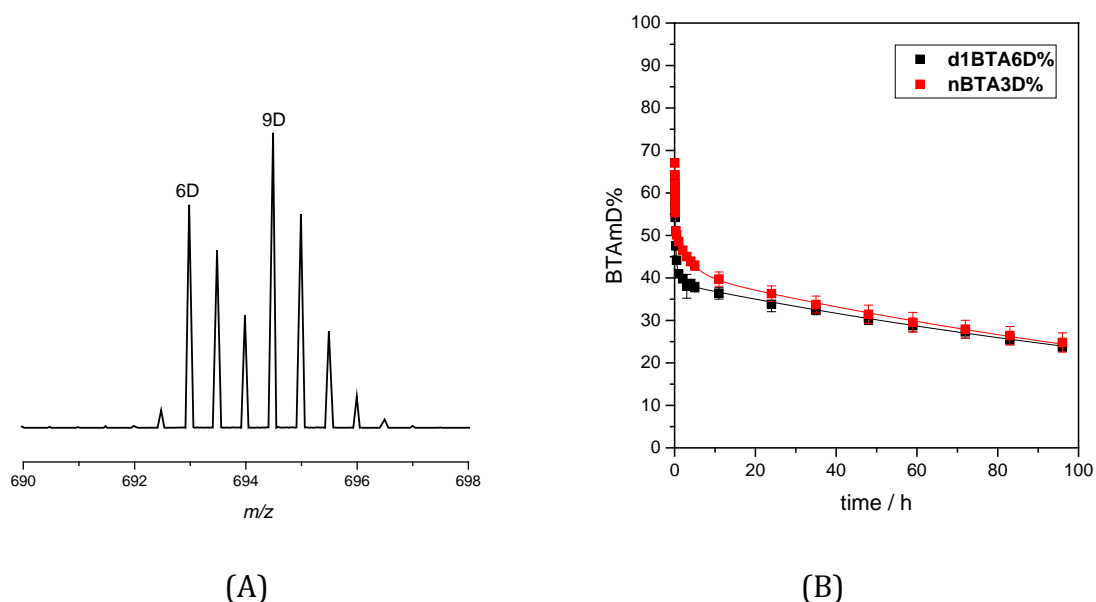


Figure S18: (A) HDX-MS of **d1BTA** (1333.97 g/mol) in which one distribution corresponds to $[\text{d1BTA6D} + 2\text{Na}]^{2+}$ and the second to $[\text{d1BTA9D} + 2\text{Na}]^{2+}$. For this, a 500 μM solution in H_2O was diluted 100 times in D_2O , and a sample was injected after $t = 1$ h; (B) HDX-MS of **d1BTA** and **nBTA**

followed as a function of time in which the percentage of **nBTA3D** (red data) or **d1BTA6D** (black data) is probed.

4. Preparation procedures for aqueous BTA samples

Samples of the BTA derivatives for all measurements were prepared by adding the appropriate amount of milliQ water to the desired BTA or mixtures of BTAs weighted into a sample vial. The sample was then heated at 75°C for 1 h. Halfway the heating, the sample was vortexed for 15 sec.

5. HDX measurements

HDX-MS is a well-known technique to probe the structure and folding processes in proteins.³ We here performed the HDX-MS experiments of **dBTA** and compared the results to those obtained with **nBTA**. Hereto, 500 μM solutions of **nBTA** or **dBTA** were prepared in water and 100 times diluted in D_2O . At this 20-fold lower concentration, the UV signature of both solutions remained identical to that measured at 100 μM (Figure S16) indicating that the nature of the aggregates does not change. All the BTA molecules studied here have three amide hydrogens at the core and different numbers of hydroxyl hydrogens at the glycol-based peripheries. Only these hydrogen atoms are able to undergo H \rightarrow D exchange (HDX) reactions with the surrounding water. The H/D exchange rate depends on the solvent accessibility to these exchangeable hydrogens. This rate is fast for the OH groups in both the aggregates formed by **dBTA** as well as supramolecular polymers formed by **nBTA** because the hydrophilic glycol-based motifs remain fully exposed to the surrounding solvent. As a result, HDX of the hydroxyl groups does not provide any information on the exchange dynamics of the supramolecular aggregates. The amide NH groups, on the other hand, can be buried inside a supramolecular aggregate as a result of the formation of a hydrophobic pocket. Consequently, the H/D exchange rate slows down. The H/D exchange dynamics of the amide-NHs are therefore connected to the exposure of the amide-NHs into the surrounding aqueous medium by dynamic exchange of monomers between polymers. As a result, the increase in the molar mass of the molecule by replacing NH to ND is a direct measure of the exchange dynamics of monomers between supramolecular polymers.

Upon diluting a BTA- H_2O solution 100 times into D_2O , all the hydrogens of the OH groups at the periphery will be instantaneously replaced by deuterium leading to the immediate transformation of BTA to BTAmD (m is the number of OH groups at the periphery in a BTA molecule). Subsequently, HDX of the three amide groups will take place forming $\text{BTA}(m+3)\text{D}$.⁴ In calculating the percentage of BTA molecules with the amide hydrogens not exchanged by deuterium, the overlapping isotopic peaks of BTAmD and $\text{BTA}(m+3)\text{D}$, and the presence of 1% H_2O (w/w, with molar ratio of 1.1%), should be taken into account. Considering the presence of 1.1% (molar ratio) of H_2O in a HDX solution, all hydrogen atoms (m OH and 3 NH) cannot be completely replaced by deuterium. Statistically, the ratios of $\text{BTA}(m+1)\text{D} : \text{BTA}(m+2)\text{D} : \text{BTA}(m+3)\text{D}$ are, $[(m+3) \times (m+2) / 2] \times (1.1 \times 10^{-2})$

²)² : (m+3)×1.1×10⁻² : 1. Although the amount of BTA(m+1)D formed is negligible (0.185% for nBTA4D and 1.3% for dBTA13D), the amount of BTA(m+2)D (6.6% for nBTA5D and 16.5% for dBTA14D) has to be taken into consideration when calculating the percentage of BTAmD. Based on the discussion above, BTAmD% is calculated by the following equation,

$$BTAmD\% = \frac{I_{BTAmD}}{I_{BTAmD} + (I_{BTA(m+3)D} - p \times I_{BTAmD}) \times (1 + (m + 3) \times 1.1\%)} \times 100$$

where I_{BTAmD} and $I_{BTA(m+3)D}$ represent the intensities of the monoisotopic peaks for the sodiated ions of BTAmD and BTA(m+3)D, and p is the relative isotopic peak intensity at mass of M_0+3 (M_0 is the monoisotopic mass of BTAmD, $p = 0.104$ for nBTA and $p = 0.126$ for dBTA) contributed from BTAmD.

6. Fit Procedure

Non-linear least squares weighted optimizations of the HDX data were performed with a tri-exponential decay curve (Eq. 2) using the *lsqcurvefit* function from the Matlab software package (R2016a, version 9.0.0341360, Mathworks, optimization toolbox). This function uses the Levenberg-Marquardt method to minimize the residual sum of squares. A thousand fits were performed for each optimization. Initial parameters for the fits were distributed using latin hypercube sampling (implemented in the *lhsdesign* function), which ensures a uniform distribution in multidimensional parameterspace so that the global optimum can be obtained. The optimization with the lowest squared 2-norm is used as the best fit. Estimates of the standard deviations on the optimized parameters were generated from the Jacobian and normalized residuals.⁵

$$y = a_1 e^{-k_1 t} + a_2 e^{-k_2 t} + a_3 e^{-k_3 t} \quad (2)$$

Where y is the percentage of deuterium exchanged, a is the pre-exponential factor, k is the time constant and t is the time.

7. Matlab script for tri-exponential curve fitting of HDX decay data

```
function HDX_fit
%6 curves, 4 models, 1000*24 fits
close all;clear all;
load('LastFit_1000_nBTA.mat')
% load('LastFit_1000_nBTA_no_t0.mat')
% load('LastFit_1000_dBTA.mat')
% load('LastFit_1000_dBTA_no_t0.mat')
flag_calc = 0;
while flag_calc == 1;
    %% import data
    load('data160915_nBTA.mat')
    % load('data161114_dBTA.mat')
    % xdata=xdata(2:end);ydata=ydata(2:end,:);ySD=ySD(2:end,:); %exclude first point
    %% parameters
    J=1e3; %number of fits
    numpar=7; %number of fit parameters
    J1=lhsdesign(J,numpar);
    options=optimset('MaxIter',100,'Display','Off','MaxFunEvals',1000,...
        'TolX',1e-9,'TolFun',1e-9);
    R=Inf*ones(4,6);h=waitbar(0,'Performing fits');
    F=zeros(7,J,4,6);resnorms=zeros(J,4,6);
```

```

functions={'biexp','biexp_offset','triexp','triexp_offset'};
for j=1:J
    waitbar((j-1)/J,h,sprintf('Performing fit %1.0f of %1.0f. Overall progress:',j,J));
    for a=1:6 %curves
        yin=ydata(:,a);
        yweights=1./ySD(:,a);
        yweights(1)=2;
        for b=1:4 %functions
            if b==3
                %custom bounds for triexp to order parameters
                lb(2)=5;      ub(2)=1e2;      g0(:,2)=10.^((J1(:,2).*log10(100-5+1)))+4;
                lb(4)=0.1;   ub(4)=5;        g0(:,4)=10.^((J1(:,4).*log10(5-0.1+1)))-0.9;
                lb(6)=0;     ub(6)=0.1;     g0(:,6)=10.^((J1(:,6).*log10(0.1-0+1)))-1;
            else
                ub= repmat([100 Inf],1,4);
                lb=zeros(1,numpar);
                g0=[J1(:,1)*100 10.^((J1(:,2).*20)-10) J1(:,3)*100 10.^((J1(:,4).*20)-10)
J1(:,5)*100 10.^((J1(:,6).*20)-10) J1(:,7)*100]; %vector of initial guesses
            end
        end

eval(['[A.par,A.resnorm,A.residual,A.exitflag,A.output,A.lambda,A.jacobian]=lsqcurvefit(@(fitpar,xdata) ' functions{b}
'(fitpar(1:b+3),xdata,yweights),g0(j,1:b+3),xdata,yin.*yweights,lb(1:b+3),ub(1:b+3),options);'])
        if A.resnorm < R(b,a); %store best fit
            bestfit{b,a}=A;
            R(b,a)=A.resnorm;
        end
        F(1:b+3,j,b,a)=A.par';
        resnorms(j,b,a)=A.resnorm;
    end
end
waitbar(j/J,h)
end
close(h)

%% post-fit analysis
for a=1:6 %curves
    for b=1:4 %functions
        I{b,a}=find(resnorms(:,b,a)<=1.05*bestfit{b,a}.resnorm); %detect which parameter sets
give best values. resnorm <= 5% of best fit
        %calculate pearson correlation coefficient matrix
        C = inv(full(bestfit{b,a}.jacobian)'*full(bestfit{b,a}.jacobian));
        corr_mat{b,a} = C./sqrt(diag(C)*diag(C)');
        %calculate 95% confidence intervals on fit parameters
        conflvel=0.05;

ci=nlparci(bestfit{b,a}.par,bestfit{b,a}.residual,'Jacobian',bestfit{b,a}.jacobian,'alpha',conflvel);

        tsd=tinv(1-conflvel/2,length(bestfit{b,a}.residual)-length(bestfit{b,a}.par));
        par_sd=(ci(:,2)-ci(:,1))./(2*tsd);
        bestfit{b,a}.par=bestfit{b,a}.par';
        bestfit{b,a}.par=[bestfit{b,a}.par par_sd];
        clear C ci tsd par_sd
    end
end
% calculate F test value
df=[18 17 16 15];
for a=1:6 %curves
    for b=2:4 %functions
        Ftest(b,a)=(bestfit{b-1,a}.resnorm -bestfit{b,a}.resnorm)/bestfit{b,a}.resnorm/((df(b-1)
-1) -df(b))/df(b);
        p(b,a)=fpdf(Ftest(b,a),df(b),(df(b-1)-df(b)));
    end
end
% save results
save(sprintf('LastFit_%1.0f_nBTA.mat',J))
% save(sprintf('LastFit_%1.0f_dBTA_no_t0.mat',J))
flag_calc=0;
end

%% visualize
titles={'nBTA','2:1 nBTA:dBTA','1:1 nBTA:dBTA','1:2 nBTA:dBTA','1:1 C10:C12 nBTA','1:1 nBTA:d1BTA'};
functions={'biexp','biexp_offset','triexp','triexp_offset'};
functitles={'BiExp','BiExp + y0','TriExp','TriExp + y0'};
label={'A1','k1','A2','k2','A3','K3'};
markers={'-x','--o','-s',':d'};
% plot data and best fit

```

```

locfunc=[1 2 5 6];
for a=1:6 %curves
    figure(a+3);
    for b=1:4 %functions
        subplot(2,4,locfunc(b));hold on;
        plot(xdata,eval([functions{b},'(bestfit{b,a}.par(:,1),xdata,ones(size(xdata)))']), '-r')
        errorbar(xdata,ydata(:,a),ySD(:,a),'o','LineWidth',2)
        set(gca,'XScale','log','XLim',[0.05 100]) %,'YLim',[0 100])
%         set(gca,'XScale','linear','XLim',[0 100],'YLim',[0 100])
        title(functiontitles{b})
        if b>1; text(10,70,sprintf('F = %2.0f\np = %1.1e',Ftest(b,a),p(b,a))); end

        subplot(2,4,3);hold on;
        plot(xdata,bestfit{b,a}.residual,markers{b}, 'Displayname',functiontitles{b})
        set(gca,'XScale','log','XLim',[0.05 100])
        title('Residuals')
        legend('Location','best')
    end
    subplot(2,4,4)
    errorbar(1:3,bestfit{3,a}.par([2 4 6],1),bestfit{3,a}.par([2 4 6],2),'s')
    set(gca,'YScale','log','FontSize',12,'XTick',1:3,'XTickLabel',label([2 4 6]))
    title('Bestfit timeconstant')

    subplot(2,4,7)
    bh = boxplot(F([1 3 5]),I{3,a},3,a),'label',label([1 3 5]),'outliersize',3,'width',.8);
    set(bh(:,:),'linewidth',2)
    h = findobj(gca, 'type', 'text');
    for j=1:length(h)
        set(h(j),'Position',get(h(j),'Position')+[0 -5 0]);
    end
    set(gca,'FontSize',12)%,'Ylim',[8e4 8e7])
    title('Parval pre-exp')

    subplot(2,4,8)
    bh = boxplot(F([2 4 6]),I{3,a},3,a),'label',label([2 4 6]),'outliersize',3,'width',.8);
    set(bh(:,:),'linewidth',2)
    h = findobj(gca, 'type', 'text');
    for j=1:length(h)
        set(h(j),'Position',get(h(j),'Position')+[0 -5 0]);
    end
    set(gca,'YScale','log','FontSize',12)
    title('Parval timeconstant')
    suptitle(titles{a});
end

%plot bestfit parameter values versus %nBTA
% xdat=[0 33.33 50 66.66];
xl=length(xdat);
for a=1:6 %curves
    parvals(:,a)=bestfit{3,a}.par(:,1);
    parsd(:,a)=bestfit{3,a}.par(:,2);
end
figure;
subplot(2,2,1);hold on;
for a=[1 3 5]; errorbar(xdat,parvals(a,1:xl),parsd(a,1:xl), '-s'); end
set(gca,'FontSize',12,'XLim',[-2 100])
xlabel('dBTA [%]')
title('Bestfit pre-exponential terms')

subplot(2,2,2);hold on;
for a=[1 3 5]; errorbar(1:6-xl,parvals(a,xl+1:6),parsd(a,xl+1:6), 's'); end
set(gca,'FontSize',12,'XTick',1:6-xl,'XTickLabel',titles(xl+1:6))%,'XTickLabelRotation',-20)
title('Bestfit pre-exponential terms')

subplot(2,2,3);hold on;
for a=[2 4 6]; errorbar(xdat,parvals(a,1:xl),parsd(a,1:xl), '-s'); end
set(gca,'YScale','log','FontSize',12,'XLim',[-2 100])
xlabel('dBTA [%]')
title('Bestfit timeconstants')

subplot(2,2,4);hold on;
for a=[2 4 6]; errorbar(1:6-xl,parvals(a,xl+1:6),parsd(a,xl+1:6), 's'); end
set(gca,'YScale','log','FontSize',12,'XTick',1:6-xl,'XTickLabel',titles(xl+1:6))
title('Bestfit timeconstants')

%plot exponential contributions for each curve

```

```

figure;
for a=1:6
    subplot(2,3,a);hold on;
    for c=1:3
        p1=bestfit{3,a}.par((c-1)*2+1,1);
        p2=bestfit{3,a}.par(c*2,1);
        plot(xdata,p1.*exp(-p2.*xdata),'-','LineWidth',2)
    end
    errorbar(xdata,ydata(:,a),ySD(:,a),'o','LineWidth',2)
    set(gca,'XScale','log','XLim',[0.05 100])
    xlabel('Time [hours]')
    title(titles{a})
end

%compare dBTA and nBTA best fit parameters
figure;hold on;
colors=lines(3);
for d=1:2
    if d==1; load('LastFit_1000_nBTA.mat'); x=[1 3]; else load('LastFit_1000_dBTA.mat'); x=1:3; end
    xl=length(xdat);
    linestyle={'-','--'};
    markerstyles={'square','diamond'};
    for a=1:6 %curves
        parvals(:,a)=bestfit{3,a}.par(:,1);
        parsd(:,a)=bestfit{3,a}.par(:,2);
    end
    subplot(2,2,1);hold on;count=1;
    for a=[1 3 5];
        errorbar(xdat,parvals(a,1:xl),parsd(a,1:xl),'Marker',markerstyles{d},'LineStyle',linestyle{d},'Color',
r',colors(count,:));count=count+1; end
        set(gca,'FontSize',12,'XLim',[-2 100])
        xlabel('dBTA [%]')
        title('Bestfit pre-exponential terms')

        subplot(2,2,2);hold on;count=1;
        for a=[1 3 5];
            errorbar(x,parvals(a,xl+1:6),parsd(a,xl+1:6),'Marker',markerstyles{d},'LineStyle','none','Color',col
ors(count,:));count=count+1; end
            set(gca,'FontSize',12,'XTick',1:6-xl,'XTickLabel',titles(xl+1:6))%,'XTickLabelRotation',-20)
            title('Bestfit pre-exponential terms')

            subplot(2,2,3);hold on;count=1;
            for a=[2 4 6];
                errorbar(xdat,parvals(a,1:xl),parsd(a,1:xl),'Marker',markerstyles{d},'LineStyle',linestyle{d},'Color'
r',colors(count,:));count=count+1; end
                set(gca,'YScale','log','FontSize',12,'XLim',[-2 100])
                xlabel('dBTA [%]')
                title('Bestfit timeconstants')

                subplot(2,2,4);hold on;count=1;
                for a=[2 4 6];
                    errorbar(x,parvals(a,xl+1:6),parsd(a,xl+1:6),'Marker',markerstyles{d},'LineStyle','none','Color',col
ors(count,:));count=count+1; end
                    set(gca,'YScale','log','FontSize',12,'XTick',1:6-xl,'XTickLabel',titles(xl+1:6))
                    title('Bestfit timeconstants')
                end
            end

function y=biexp(fitpar,time,weights)
y=(fitpar(1)*exp(-fitpar(2)*time) +fitpar(3)*exp(-fitpar(4)*time)).*weights;
end
function y=biexp_offset(fitpar,time,weights)
y=(fitpar(1)*exp(-fitpar(2)*time) +fitpar(3)*exp(-fitpar(4)*time) +fitpar(5)).*weights;
end
function y=triexp(fitpar,time,weights)
y=(fitpar(1)*exp(-fitpar(2)*time) +fitpar(3)*exp(-fitpar(4)*time) +fitpar(5)*exp(-
fitpar(6)*time)).*weights;
end
function y=triexp_offset(fitpar,time,weights)
y=(fitpar(1)*exp(-fitpar(2)*time) +fitpar(3)*exp(-fitpar(4)*time) +fitpar(5)*exp(-fitpar(6)*time)
+fitpar(7)).*weights;
end
function y=biexp_burst(fitpar,time,weights)
y=(100- (fitpar(1)*(1-exp(-fitpar(2)*time)) +fitpar(3)*(1-exp(-fitpar(4)*time))
+fitpar(5))).*weights;
end

```

8. Molecular dynamics simulations

The entire simulation work was conducted with the AMBER 14 software.⁶ The atomistic models for the water-soluble **nBTA** monomer and homopolymer were taken from our previous work.⁷ The molecular model for the branched water-soluble **dBTA** monomer was built and parametrized accordingly, based on the general AMBER force field (GAFF) (*gaff.dat*).⁸ The atomistic models for the 2:1 **nBTA:dBTA** copolymer was built starting from the initially extended one for the **nBTA** homopolymer reported recently,⁷ and replacing the side chains in order to have one extended **dBTA** every two **nBTA** monomers. In this model,⁷ 48 extended monomers (32 **nBTA** and 16 **dBTA** alternated in a 2:1 fashion) have the cores prestacked in a configuration pre-optimized by means of density functional theory calculations in vacuum (intercore distance of 3.4 Å).⁸ The atomistic copolymer model was immersed in a periodic simulation box containing explicit TIP3P water molecules⁹ As previously done for homopolymers,⁷ the simulation box for the copolymer model was designed grazing the terminal cores in the direction of the *z* axis (main axis of the copolymer). Replicated in space through periodic boundary conditions, this molecular model is representative of a section of the bulk of an ideal copolymer of infinite length where **dBTA** and **nBTA** monomers are uniformly mixed. After initial minimization, the copolymer model was first heated through 50 ps of MD simulation in NVT conditions (constant N: number of atoms, V: volume and T: temperature) to reach the experimental temperature of 20 °C keeping the solute fixed. Then, the restraints on the lateral chains of the monomers were removed and the side chains of the monomers were relaxed in water for 2 ns of MD simulation in NPT conditions (constant N: number of atoms, P: pressure and T: temperature) at room temperature (*T*=20 °C) and 1 atm of pressure using anisotropic pressure scaling. After these preliminary phases, all restraints were removed and the copolymer was relaxed for 400 ns of MD simulation in NPT conditions at 20 °C of temperature and 1 atm of pressure in the same conditions. A time step of 2 fs was used in the MD run, together with the Langevin thermostat and an 8 Å cutoff. We used the particle mesh Ewald¹⁰ approach to treat the long-range electrostatics and the SHAKE algorithm for all bonds involving Hydrogen atoms.¹¹ During the run, the copolymer model successfully reached the equilibration in the MD regime. The last 100 ns of MD simulations were used for data analysis. All analyses (*g(r)*, SASA, etc.) were performed as in our previous works.^{7,12}

We also built and simulated a system containing 32 **nBTA** and 16 **dBTA** pre-arranged in segregated domains (Figure S18). However, the same analyses on this system demonstrated no difference in all **nBTA** assembly parameters compared to the **nBTA** homopolymer, suggesting that indeed in reality the **nBTA** and **dBTA** monomers tend to mix uniformly rather than creating compartmentalized

domains. In fact, in such a case, the structural packing of the **nBTA** monomers in the copolymer would be nearly identical to that of a **nBTA** homopolymer, which would produce the same dynamics of a **nBTA** homopolymer instead of the decreased dynamics seen in the experiments.

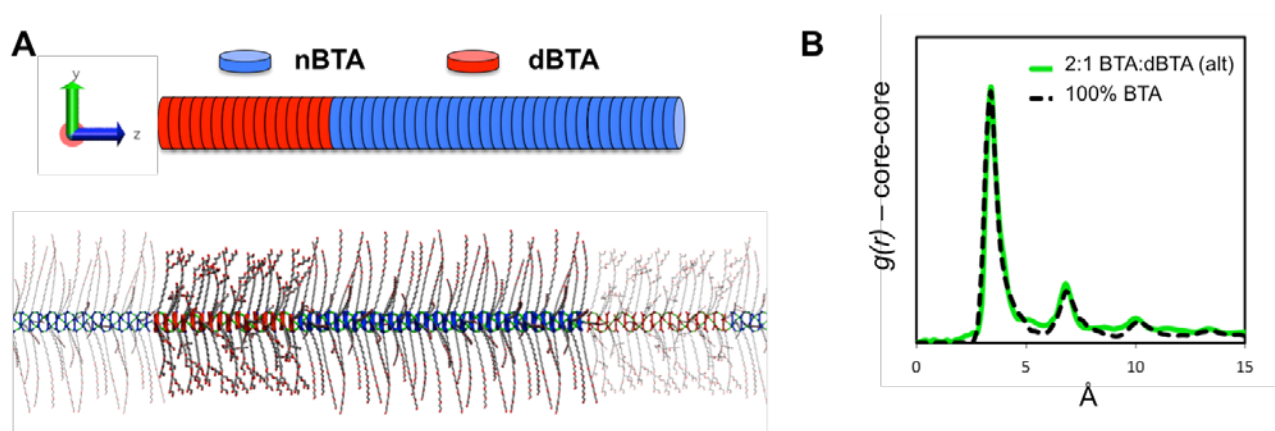


Figure S19: All-atom molecular dynamics (MD) simulations of a 2:1 **nBTA**:**dBTA** copolymer where the **nBTA** and **dBTA** monomers are initially arranged in compartmentalized domains. (A) Initial configuration for the copolymer, which was then relaxed and equilibrated in water. (B) Core-core radial distribution functions ($g(r)$) for the **nBTA** homopolymer (black) and the 2:1 **nBTA**:**dBTA** “alternated” copolymer (green).

9. References

- [1] C. M. A. Leenders, L. Albertazzi, M. Koenigs, A. R. A. Palmans, E. W. Meijer, *Chem. Commun.* **2013**, 49, 1963–1965.
- [2] M. L. Ślęczkowski, E. W. Meijer, A. R. A. Palmans, *Macromol. Rapid Commun.*, **2017**, DOI: 10.1002/marc.201700566.
a) D. L. Smith, Y. Deng, Z. J. Zhang, *Mass Spectrom.* **1997**, 32, 135–146; b) T. E. Wales, J. R. Engen, *Mass Spectrom. Rev.*, 2006, 25, 158–170; c) S. W. Englander, *Annu. Rev. Biophys. Biomol. Struct.*, **2000**, 29, 213–238; d) L. Konermann, J. Pan, Y.-H. Liu, *Chem. Soc. Rev.*, 2011, 40, 1224–1234.
- [4] X. Lou, R. P. M. Lafleur, J. L. J. van Dongen, C. M. A. Leenders, M. B. Baker, A. R. A. Palmans, E. W. Meijer, *Nat. Commun.* **2017**, 8, 15420.
- [5] W. H. Press, B. P. Flannery, S. A. Teukolsky, W. T. Vetterling, *Numerical Recipes in C: The Art of Scientific Computing*, 2nd edition; Cambridge University Press: Cambridge ; New York, 1992.
- [6] D.A. Case, V. Babin, J.T. Berryman, R.M. Betz, Q. Cai, D.S. Cerutti, T.E. Cheatham, T.A. Darden, R.E. Duke, H. Gohlke, A.W. Goetz, S. Gusarov, N. Homeyer, P. Janowski, J. Kaus, I. Kolossváry, A. Kovalenko, T.S. Lee, S. LeGrand, T. Luchko, R. Luo, B. Madej, K.M. Merz, F. Paesani, D.R. Roe, A. Roitberg, C. Sagui, R. Salomon-Ferrer, G. Seabra, C.L. Simmerling, W. Smith, J. Swails, R.C. Walker, J. Wang, R.M. Wolf, X. Wu and P.A. Kollman (**2014**), AMBER 14, University of California, San Francisco
- [7] a) M. B. Baker, L. Albertazzi, I. K. Voets, C. M. A. Leenders, A. R. A. Palmans, G. M. Pavan, E. W. Meijer, *Nat. Commun.* **2015**, 6, 6234; b) M. Garzoni, M. B. Baker, C. M. A. Leenders, I. K. Voets, L. Albertazzi, A. R. A. Palmans, E. W. Meijer, G. M. Pavan, *J. Am. Chem. Soc.* **2016**, 138, 13985–13995.
- [8] J. Wang, R. M. Wolf, J. W. Caldwell, P. A. Kollman, D. A. Case, *J. Comput. Chem.* **2004**, 25, 1157–1174.
- [9] W. L. Jorgensen, J. Chandrasekhar, J. D. Madura, R. W. Impey, M. L. Klein, *J. Chem. Phys.* **1983**, 79, 926–935.
- [10] T. Darden, D. York, L. Pedersen, *J. Chem. Phys.* **1993**, 98, 10089–10092.
- [11] V. Krättiler, W. F. van Gunsteren, P. H. Hunenberger, *J. Comput. Chem.* **2001**, 22, 5385–5399.
- [12] D. Bochicchio, M. Salvalaglio, G. M. Pavan, *Nature Commun.* **2017**, 8, 147.